Racemic alkylamides of *trans*-cyclohexane-β-amino acids surpass the gelation ability of their pure enantiomers. From macroscopic behavior to microscopic structure

David Reza,[a] Víctor M. Sánchez-Pedregal,[b] Bruno Dacuña,[c] Ramón J. Estévez[a,b] and Juan C. Estévez[a,b,*]

[a] Centro Singular de Investigación en Química Biolóxica e Materiais Moleculares (CiQUS), Universidade de Santiago de Compostela, Rúa Jenaro de la Fuente s/n, 15782 Santiago de Compostela, Spain

[b] Departamento de Química Orgánica, Universidade de Santiago de Compostela, Avda. das Ciencias s/n, 15782 Santiago de Compostela, Spain

[c] Servizo de Raios-X, RAIDT, Universidade de Santiago de Compostela, Rúa de Constantino Candieira 1. 15782 Santiago de Compostela, Spain

* Corresponding author: Juan C. Estévez, juancarlos.estevez@usc.es

Abstract

We describe the excellent gelation capabilities of amides derived from *trans*-cyclohexane-β-amino acid, demonstrating their great potential to generate lypogels in a wide variety of solvents. Structural factors affecting this behavior, like modifying the balance between their hydrophilic/hydrophobic moieties (by changing their alkyl chain length) or their enantiomeric composition (enantiomerically pure compounds *vs*. racemic mixtures) were investigated. A comprehensive structural analysis ranging from microscopic arrangements to their macroscopic structures is also discussed.

INTRODUCTION

Gels are known since ancient times and have been the subject of intense studies due to their continuous presence in Nature.[1] as well as their important applications.[2] However, data on their structuring at the molecular level are limited, probably because of the complexity of the macromolecular networks, that can be linked by covalent bonds

(chemical gels), by association of macromolecules through weak bonding forces, or by self-organization of small molecules (LMWOGs) into physical polymers bound by weak bonding forces (physical gels).[3] In all cases the gelation is accompanied by a complicated and not very well defined network of intermolecular associations difficult to determine.[4] Besides, especially in the case of physical gels, those interactions are not static and can change after formation of the gel in response to external variables like time, heat, stress, and others.[5] Therefore, gels do not lend themselves to being studied by traditional methods that offer precise structural information such as X-ray techniques. However, this has changed favorably in recent years with the emergence of techniques that render fairly precise structural information on the structuring of gels, such as powder X-ray diffraction (PXRD).[6]

In the last three decades, LMWOGs have received special attention by the scientific community, not only because of their capability to self-organize, giving rise to physical polymers without the need for chemical synthesis of a previous polymeric chain, but also because of the ease with which their three-dimensional network can be formed and reversed.[7] Studies carried out in the LMWGs have always paid special attention to the presence of structural motifs that can participate in weak intermolecular bonding interactions (mainly H-bonds, Van der Waals forces, π stacking, hydrophobic or hydrophilic interactions), because those interactions are always necessary to achieve the formation of gels.[3,8] However, less attention has been paid to the characteristics of the molecules that must accompany the above in order to achieve a good gelation agent, such as the rigidity of their structure, the proportion of hydrophilic/hydrophobic moieties in the molecule, or their chirality.[9]

Regarding the suitable functional groups for generating the three-dimensional network of gels, particular interest has been shown in chemical groups capable of establishing strong polar interactions depending on the medium, such as amines and carboxylic acids, but also amides, urethanes or ureas with N-H and C=O bonds capable of establishing a network of H-bonds between them. As far as the rigidity of the molecules is concerned, cyclic molecules, generally cyclohexanes, have been chosen for their excellent conformational properties, but other types of cycles and even polycycles have

been studied and have also shown very good gelation properties. The balance between hydrophilicity and hydrophobicity has usually been proposed by means of alkyl chains of different lengths.

Chirality is not a necessary requirement for gelation but has to be considered because there are many gelators that are chiral. The influence of the chirality of the LMWOGs on the formation of a gel has almost always focused on ordered systems consisting of a pure isomer, and much less often on systems consisting of mixtures of isomers or racemates.[10] The reason is the observation that enantiomerically pure compounds lead to more ordered systems and, therefore, better gelation properties, while racemates usually lead to less ordered systems, with poorer or no gelation ability.[11] Thus, when racemic systems with good gelation properties have been found, it has been interpreted that their greater disorder contributed to networks capable of accommodating more solvent. This general consideration is based on a partial interpretation of Pasteur's postulates[12] considering that the racemates can be ordered to form separately physical polymers equal to those that would form their pure enantiomers, although with more difficulty or even with the impossibility of giving rise to a network capable of generating the gel. This interpretation fails to notice the possibility that the two enantiomers are ordered at the molecular level (true racemate) or that the physical polymers generated by each of them associate with each other. In both cases the supramolecular ordering of the racemate would be different from that of each of the pure compounds and therefore their gelation properties should be different too.

As we have already anticipated, among a plethora of synthetic LMWGs systems described, cyclohexanic ring derivatives are one of the most important classes, because the carbocyclic ring can act as a chemical platform bearing suitable functional groups in precise orientations, such as amide, urea or acid, which are able to form H-bonds, as well as long alkyl chains or aromatic systems favoring molecular stacking. Furthermore, in these molecules, chirality, in conjunction with conformational restriction due to the ring strain, is a powerful tool to promote and direct the aforementioned interactions leading to aggregates.[13] Within this group of LMWGs, alkylamides derived from 1,2-diaminocyclohexanes have been extensively studied, as they show excellent gelation

properties.[14] Alkylamides derived from 1,2-cyclohexanedicarboxylic acids have also been studied and have shown much more modest gelling properties.[15,16] Surprisingly, alkylamides derived from 2-aminocyclohexanecarboxylic acids (cyclohexane-β-amino acids) have received virtually no attention to our knowledge, even though gelling systems based on α-amino acids have been the subject of extensive studies in the field of molecular gels.

Here we present the synthesis and the study of the gelling potential of alkylamides derived from enantiopure (1R,2R)-*trans*-2-aminocyclohexanecarboxylic acid ((1*R,2R*)-**1** and (1*R,2R*)-**2**) and from racemic (±)-*trans*-2-aminocyclohexanecarboxylic acid (*rac*-**1** and *rac*-**2**). In this study, these compounds demonstrate good to excellent gelling properties of apolar and medium polarity solvents. In fact, amide (1*R,2R*)-**1** is the best hexane gelling agent described to date. Much more important is the fact that the enantiomeric mixture *rac*-**2** surpasses dramatically the excellent gelling abilities of the enantiomerically pure (1*R,2R*)-**2**.

RESULTS AND DISCUSSION

The gelling systems we present here are constituted by compounds (1*R,2R*)-**1** and (1*R,2R*)-**2** and their enantiomeric mixtures *rac*-**1** and *rac*-**2** derived from (1*R*,2*R*)-2-((*tert*-butoxycarbonyl)amino)cyclohexane-1-carboxylic acid (**5**) and from (±)-*trans*-2-((*tert*-butoxycarbonyl)amino)cyclohexane-1-carboxylic acid (**5**+**6**) (Figure 1). Two lengths for the carboxamide N-alkyl chain were introduced: n=C_8 and n=C_{16}.

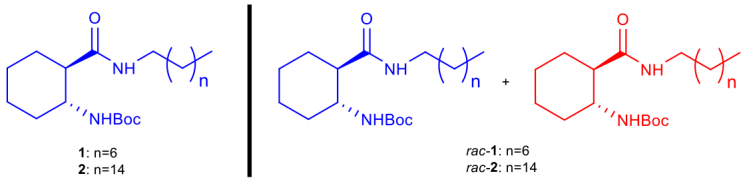

Figure 1. LMWOGs studied in this work.

Synthesis

Enantiomerically pure compounds (1*R*,2*R*)-**1** and (1*R*,2*R*)-**2** were synthesized by coupling commercially available (1*R*,2*R*)-2-((*tert*-butoxycarbonyl)amino)cyclohexane-1-carboxylic acid (**5**) with *n*-octylamine and *n*-hexadecylamine, respectively. The enantiomeric mixtures *rac*-**1** and *rac*-**2** were prepared from the commercially available racemic *trans*-2-((*tert*-butoxycarbonyl)amino)cyclohexane-1-carboxylic acid (**5**+**6**), and *n*-octylamine and *n*-hexadecylamine, respectively. This was done to demonstrate that these racemates are easily available and affordable. Detailed synthetic procedures and characterization are provided in the experimental section.

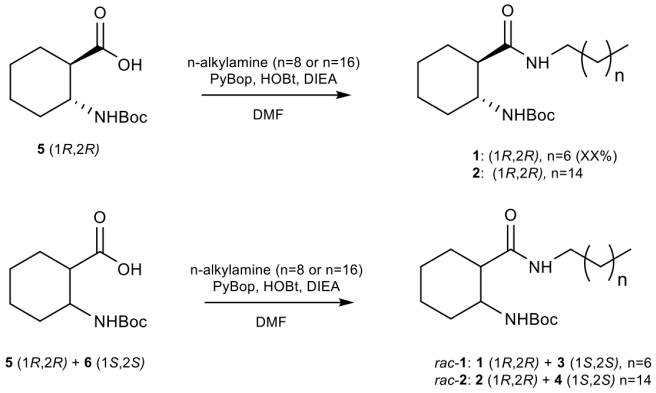

Scheme 1. Synthesis of LMWOGs.

Gelation experiments

First, we studied the scope and limitations of the capacity of these carboxamides ((1*R*,2*R*)-**1**, (1*R*,2*R*)-**2**, *rac*-**1** and *rac*-**2**) as LMWOGs by carrying out a gelation study in twelve organic solvents of different polarity by means of the inversion test (Figure 2). Water was excepted due to the low solubility of these compounds. Compound **1** is a gelling agent of six of the twelve solvents tested (less than 50 mg/mL), good for three of them (less than 10 mg/mL) and excellent for hexane (0.5 mg/mL). This is the best hexane gelling agent in the literature, to the best of our knowledge. In contrast, the enantiomeric mixture *rac*-**1** is much worse, gelling only four of the twelve solvents and with much higher minimal gelation concentration (*mgc*) than (1*R*,2*R*)-**1**, with the only exception of dioxane. Interestingly, rac-1 is still a good gelling agent for hexane.

The increase of the alkyl chain length from 8 to 16 carbon atoms causes a significant improvement in the gelling capacity of (1*R*,2*R*)-**2** with respect to ((1*R*,2*R*)-**1** for most of the solvents tested. Thus, enantiopure (1*R*,2*R*)-**2** is a gelling agent for ten of the twelve solvents tested, being good for five of them.

The behavior of *rac*-**2** is intriguing, as its gelation ability is not worse than that of the enantiomerically pure isomer (1*R*,2*R*)-**2**, as occurs with (1*R*,2*R*)-**1** and *rac*-**1**. In fact, *rac*-**2** surpasses the gelling results of (1*R*,2*R*)-**2**, being a good gelling agent for eleven of the solvents tested and also gelling toluene, a solvent that none of the three previous systems was able to gel. Regarding hexane, the result of *rac*-**2** is a little worse with respect to (1*R*,2*R*)-**1** (5 mg/mL) although it is still a good gelation agent of hexane.

The gelation results obtained with this set of carboxamides ((1*R*,2*R*)-**1**, (1*R*,2*R*)-**2**, *rac*-**1** and *rac*-**2**) show that they constitute a robust gelling system with excellent results for the gelation of hexane (compound (1*R*,2*R*)-**1**) and that it can be considered a supergelling agent in the case of *rac*-**2**. All the gels described in this article were stable for 1 month, were brought back to their sol form and regelified again, to demonstrate their stability and reversibility.

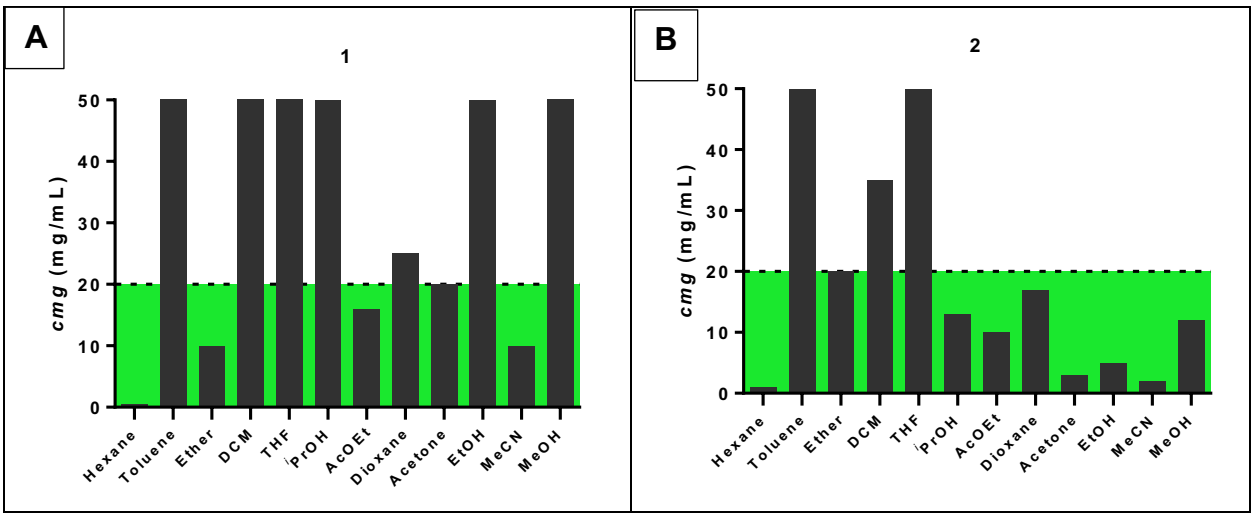

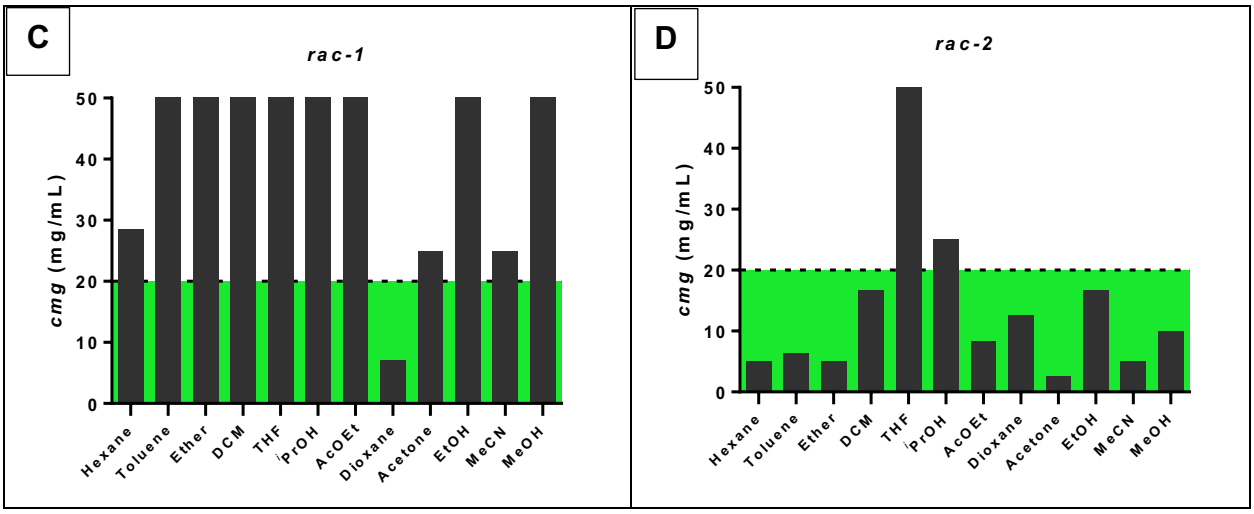

Figure 2: Gelation test showing the minimum gelation concentration (*mgc*) from 0 to 50 mg/mL for the LMWOGs (1*R*,2*R*)-**1** (A), (1*R*,2*R*)-**2** (B), *rac*-**1** (C) and *rac*-**2** (D).

In order to gain insight on the above described gelling behavior, we did a structural study of their assembly characteristics in the solid and gel states based on FT-IR, SEM, AFM and X-Ray techniques.

IR-FT Analysis

The N-H and C=O regions of the vibrational spectra of the four gelling systems (1*R*,2*R*)-**1**, (1*R*,2*R*)-**2**, *rac*-***1*** and *rac*-**2** were investigated by IR spectroscopy in solution and in the xerogel from hexane (Table 1). Bathochromic shifts ranging from 1 cm^{-1} to 7 cm^{-1} were observed in all cases, with the exception of the C=O band of (1*R*,2*R*)-**2** and the N-H band of *rac*-**2**). This suggests participation of the NH and amide C=O in H-bonding in gelation.

Table 1. IR data for the amide NH and CO bands of compounds (1*R*,2*R*)-**1**, (1*R*,2*R*)-**2**, *rac*-**1** and *rac*-**2** in solution (1 mM in MeOH/CH_2Cl_2 1:10) and in their xerogels (obtained in hexane at the *mgc*).

	NH			C=O		
	Solution	Xerogel	Bathochromic shift	Solution	Xerogel	Bathochromic shift
(1*R*,2*R*)-**1**	3331	3324	7	1647 1683	1644 1685	3 2
(1*R*,2*R*)-**2**	3333	3329	4	1645 1684	1644 1684	1 0

rac-**1**	3334	3332	2	1687 1647	1685 1646	2 1
rac-**2**	3328	3328	0	1686 1645	1684 1644	2 1

SEM Analysis

SEM images of the xerogels obtained from (1*R*,2*R*)-**1**, (1*R*,2*R*)-**2**, *rac*-***1*** and *rac*-**2** at their respective *mgc* in hexane exhibit an organization that looks more different in the size and shape of the aggregates than in the hierarchical order of them. Some selected examples are shown in Figure 3. The xerogel from enantiopure (1*R*,2*R*)-**1** is formed by fibers of 150-400 nm in size that are arranged in sheets of variable size and stacked in blocks. This gives rise to a very ordered system, which would be in accordance with its excellent capacity to gel hexane. The xerogel from *rac*-**1** also shows the association of fibers in sheets of 50-150 nm size, but they are much more irregular in shape than those from (1*R*,2*R*)-**1**, which prevents their organization in such a compact system, also in accordance with its lower capacity to gel hexane. The increase in the length of the alkyl chain in compound (1*R*,2*R*)-**2** results in the formation of fibers and lamellae, although smaller in size (50-200 nm) than those in compound (1*R*,2*R*)-**1** xerogel, and organized in a much more compact network, which could explain their capacity to gel various solvents of different dielectric constants. This tendency is much more accentuated in the case of *rac*-**2** xerogel, for which the fibers are much smaller (40-50 nm) and the network much more compact, in accordance with its behaviour as a supergelling agent.

In summary, the SEM images of (1*R*,2*R*)-**1**, (1*R*,2*R*)-**2**, *rac*-***1*** and *rac*-**2** hexane xerogels reveal that the increase in *N*-alkyl chain length leads to smaller molecular aggregates, probably due to the change in the balance between hydrophobic/hydrophyllic interactions, although with this technique it is not possible to determine the organization of the molecular network that justifies the different behavior between the enantiomerically pure and the racemates.

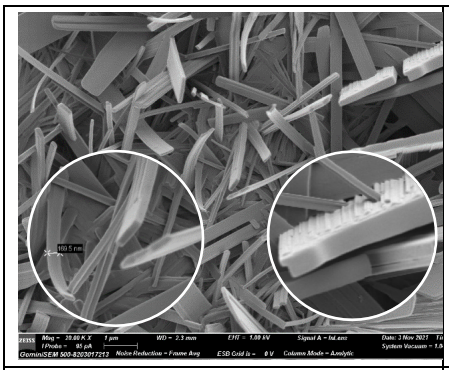

A: (1*R*,2*R*)-**1** (20K X and enlargement to 50K X**)** SEM

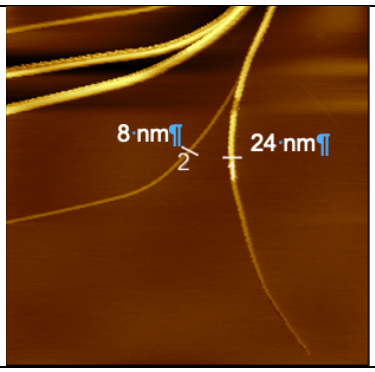

B: (1*R*,2*R*)-**1**

AFM

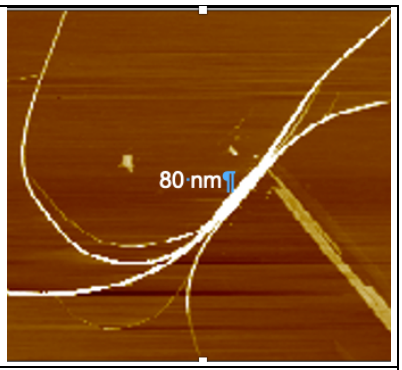

C: (1*R*,2*R*)-**1**

AFM

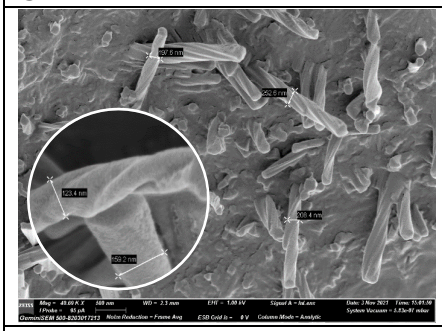

D: *rac*-**1** (40K X and enlargement to 200K X**)** SEM

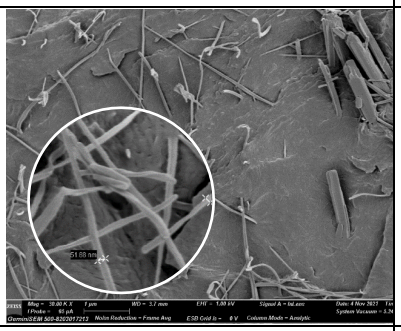

E: *rac*-**2** (30K X and enlargement to 100K X) SEM

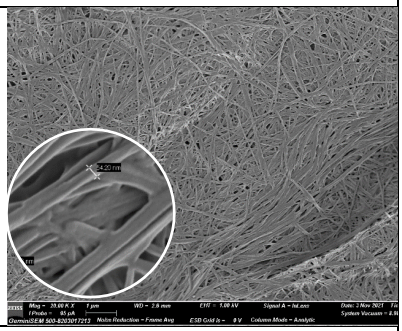

F: (1*R*,2*R*)-**2** (20K X and enlargement to 150K X) SEM

Figure 3. SEM and AFM images of hexane xerogels of (1*R*,2*R*)-**1**, (1*R*,2*R*)-**2**, *rac*-**1**, and *rac*-**2** at their *mgc*.

AFM Analysis

AFM microscopy images of compound (1*R*,2*R*)-**1** hexane xerogel (at its *mgc* in hexane) reveals very narrow fibrils, as small as 2 nm, that fit with the size of single molecule stacks (Figure 3B). Even more important than this, other images show how several of these monomeric fibres arrange in wider fibres of variable size, up to 80 nm in the experiment (Figure 3C). This size is compatible with the fibrillar arrangements observed in the SEM experiments. These images can be rationalized with a model in which (1*R*,2*R*)-**1** discrete molecules stack on top of each other to form the narrow fibril (2 nm). The wider fibers would be formed by lateral interactions of those primary fibrils.

Single-Crystal X-ray Analysis

We obtained single crystals of sufficient quality for the X-ray diffraction analysis of samples (1*R*,2*R*)-**1**, (1*R*,2*R*)-**2**, and *rac*-**1**. Their ORTEP diagrams are shown in Figure 4. Single molecule stacks interact by forming H-bonds between the amide HN and C=O group of the neighbouring molecule. The packing of the molecules in each stack follows the direction of the H-bonds in the direction of the small crystalline axis (approximately 5 Å for the three structures). The aliphatic chains of adjacent stacks interact in the plane determined by the other two crystalline axes (Figure 5).

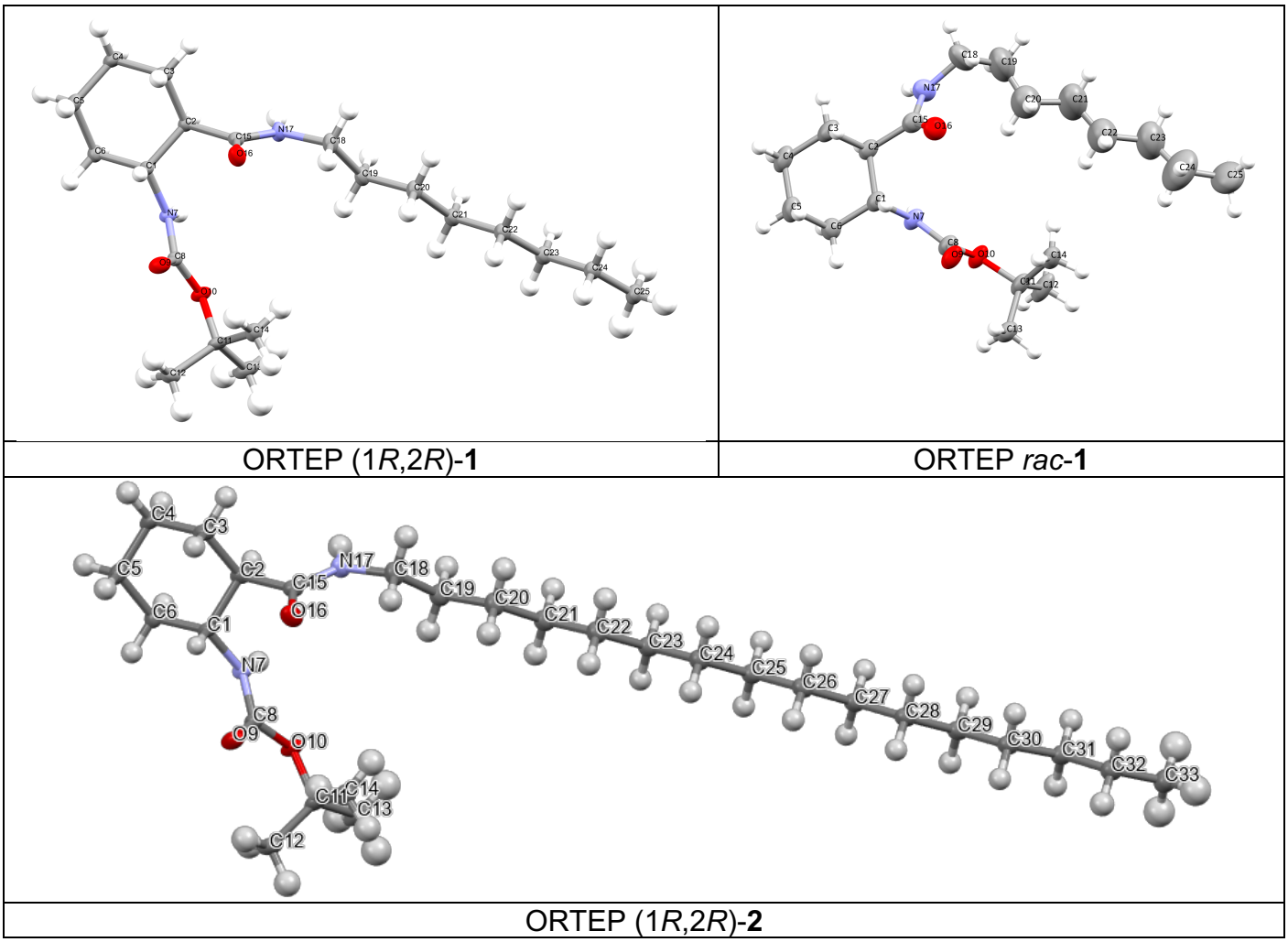

Figure 4. ORTEP diagrams for the monocrystals of (1*R*,2*R*)-**1**, (1*R*,2*R*)-**2** and *rac*-**1**.

Table 2. H-bond geometries of the single crystals of (1*R*,2*R*)-**1**, (1*R*,2*R*)-**2** and *rac*-**1**.

	D-H	A	[ARU]	d (D...H)	d (H...A)	d (D...A)	ANG(D...H...A)
1	N7 - H7	..O9	x,1+y,z	0.86(3)	2.19(3)	3.038(3)	171(2)
	N17 - H17	..O16	x,1+y,z	0.82(3)	2.05(3)	2.819(3)	156(2)
rac-1	N7 - H7	..O9	-1+x,y,z	0.86(2)	2.11(3)	2.932(3)	159(2)
	N17 - H17	..O16	-1+x,y,z	0.86(2)	2.14(3)	2.961(4)	161(2)
2	N7 - H7	..O9	x,-1+y,z	0.83(3)	2.05(4)	2.812(3)	153(3)
	N17 - H17	..O16	x,-1+y,z	0.86(4)	2.17(4)	3.021(3)	171(3)

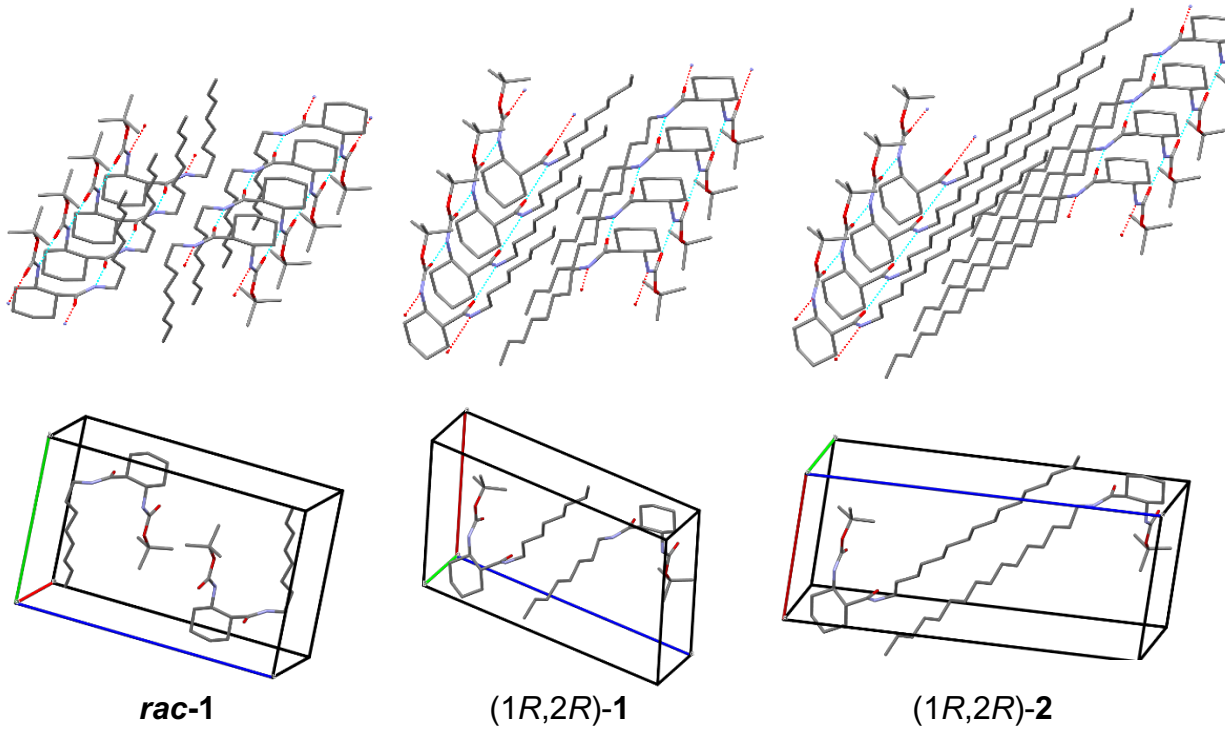

Figure 5: Packing of (1*R*,2*R*)-**1**, (1*R*,2*R*)-**2** and *rac*-**1** in their crystal structures.

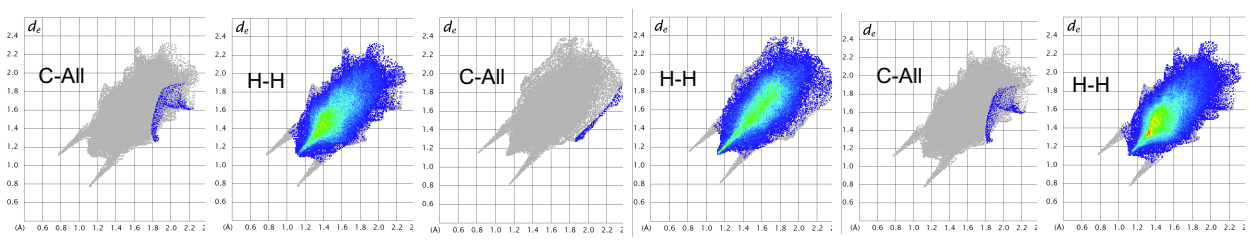

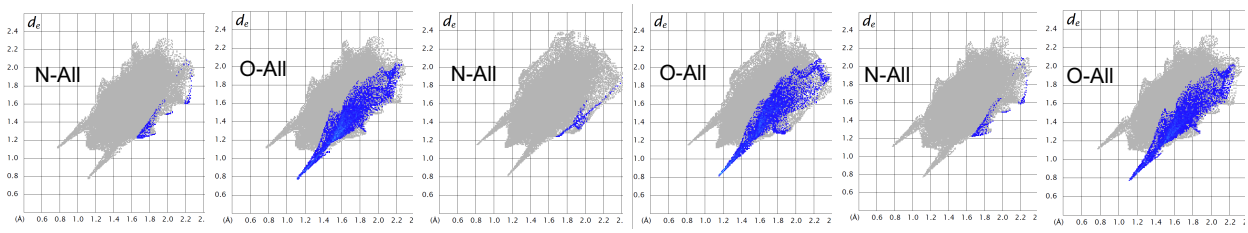

1 ***rac*-1** **2**

Figure 6: Two-dimensional representation of Hirshfeld contacts (H-H, C-All, N-All and O-All) for (1*R*,2*R*)-**1**, (1*R*,2*R*)-**2** and *rac*-**1**.

Hirshfeld surface analysis (Table 3) indicates a high percentage of Van del Waals type interactions, typical of hydrogelators (H-H contacts), and that the *O-All* contacts are the ones that provide the greatest INTER-molecular approach (H-bonds). According to the Hirshfeld surface analysis, the crystalline structure of compound (1*R*,2*R*)-**2** presents a higher proportion of H-H contacts than (1*R*,2*R*)-**1** and *rac*-**1**, which agrees with its better performance to produce gels since, as this type of non-covalent interactions have been reported to favor the immobilization of solvent molecules.[17] The formation of the extensive H-H contacts is attained without disrupting the strong H-bond contacts along the crystal minor axis.

Table 3: Hirshfeld surface contacts (H-H, H-All, C-All, N-All and O-All) for (1*R*,2*R*)-**1**, (1*R*,2*R*)-**2** and *rac*-**1**. Values are in %.

	1	***rac*-1**	**2**
	internal	**internal**	**internal**
H-All	93.2	93.5	95.0
C-All	0.5	0.3	0.3
N-All	0.3	0.3	0.2
O-All	6.1	5.9	4.5
H-H	87.8	87.5	90.5

X-ray Powder Diffraction Analysis of Xerogels

We generated four xerogels of each compound (1*R*,2*R*)-**1**, (1*R*,2*R*)-**2**, *rac*-***1*** and *rac*-**2**: two hexane xerogels (at concentrations *mgc* and 2x *mgc*) and two acetonitrile xerogels (at concentrations *mgc* and 2x *mgc*). Those solvents were chosen as examples of apolar (hexane) and polar (CH_3CN) ones. The goal was comparing the packing of the xerogels with each other and with the data obtained from the single crystals.

The powder crystal diffractograms (PXRD) of xerogel samples and the simulations of the powder crystal diffractograms from the single crystal structures are shown in Figure 7. The PXRD patterns of the (1*R*,2*R*)-**2** and *rac*-**2** xerogels are the ones that best preserve the pattern of the (1*R*,2*R*)-**2** single crystal, regardless of the solvent. In contrast, the diffractograms from the xerogels of compounds (1*R*,2*R*)-**1** and *rac*-**1** are more different from the PXRD patterns simulated from their respective monocrystals, depending also on the solvent. This suggests that their microstructure is less similar to that in the crystal.

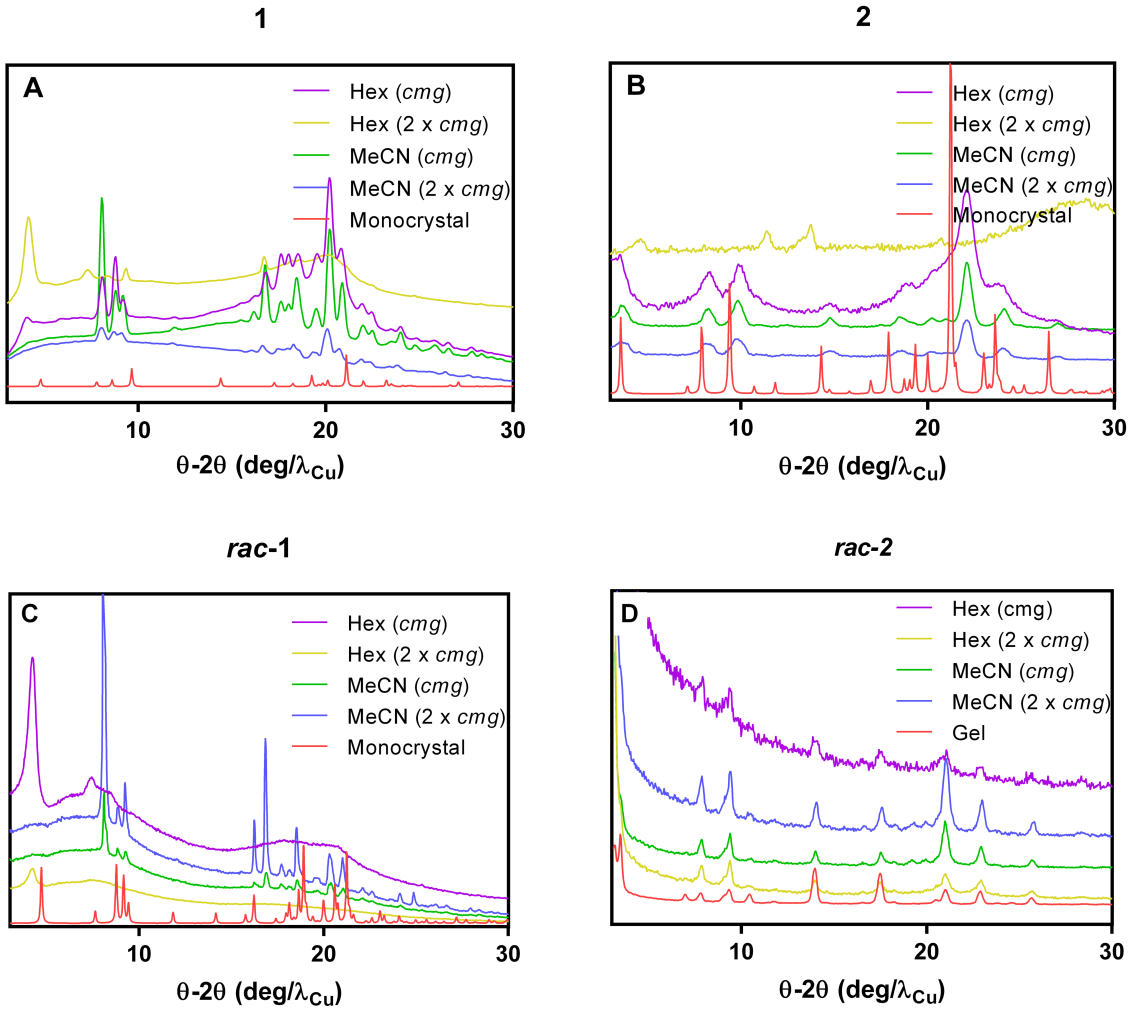

Figure 7: PXRD of hexane and CH_3CN xerogels of the four alkylamides at concentrations *mgc* and 2x *mgc*. Compounds: (1*R*,2*R*)-**1** (A), (1*R*,2*R*)-**2** (B), *rac*-**1** (C) and *rac*-**2** (D). X-Ray diffraction of the gel of *rac*-**2** in hexane (D, red line). Simulated PXRD of monocrystals for (1*R*,2*R*)-**1** (A, red line), (1*R*,2*R*)-**2** (B, red line), *rac*-**1** (C, red line).

To better visualize the behavior described above, we analyzed the metrics of the indexed cells as a function of the best PXRD diffractogram obtained for each system.[18] The Lebail analysis shows how the values of the metrics differ for each of the gelling systems (Table 4). This analysis confirms that structures (1*R*,2*R*)-**1** and *rac*-**1** show the greatest variation, while structure of (1*R*,2*R*)-**2** shows almost no structural variation. This suggests that the higher gelling power of (1*R*,2*R*)-**2**, with respect to (1*R*,2*R*)-**1** and *rac*-**1**, can be attributed to a higher degree of Van der Waals interactions for the former structure. The variation in the size of the smallest axis can be attributed, in all structures, to the flexibility of the H-bond contacts. Variations in the other axes reflect the flexibility in the contact networks of the aliphatic chains.

Table 4: Lebail metrics refinement analysis.

	1		**2**		***rac*-1**		***rac*-2**	
	monocrystal (100K)	**Indexation (298K)**	**monocrystal (100K)**	**Indexation (298K)**	**monocrystal (100K)**	**Indexation (298K)**	**monocrystal (100K)**	**Indexation (298K)**
a	11.45	11.1579	11.49	11.2476	5.0987	6.0565	-	6.393
b	5.034	5.0651	5.03	5.0802	11.6169	12.3218	-	11.629
c	18.58	22.1391	25.38	25.007	18.7828	21.0572	-	25.874
α	90	90	90	90	87.15	85.84	-	78.81
β	97.36	93.46	102.65	100.99	88.76	89.41	-	95.44
γ	90	90	90	90	86.85	85.81	-	91.56
volume	1062.1	1248.94	1430.5	1402.7	1109.27	1563.08	-	1878.5
Variations								
a	0.2921		0.2424		-0.9578		-	
b	-0.0311		-0.0502		-0.7049		-	
c	-3.5591		0.373		-2.2744		-	
α	0		0		1.31		-	
β	3.9		1.66		-0.65		-	
γ	0		0		1.04		-	
Volume	-186.84		27.8		-453.81		-	
Alifactic contacts	-2.99		0.52		-2.6		-	
H-bond	-0.07		-0.03		-0.86		-	
direction	-0.16		0.1		-0.98		-	
Perpendicular planes	0.39		0.23		5.31		-	
	-0.04		0.09		-6.08		-	

Finally, we also recorded the X-Ray diffraction of the gel of *rac*-**2** in hexane at its *mgc*, as this system is the best of the gelling agents here described. Its pattern (Figure 7D, red

line) is practically identical to that of its corresponding xerogels. This supports that extrapolation of the xerogels PXRD pattern to the corresponding gels seems reasonable.

Discussion

Here we describe for the first time the excellent gelling abilities of four gelation systems with the structure of *N*-alkylamide of 2-aminocyclohexanecarboxylic acid ((1*R*,2*R*)-**1**, (1*R*,2*R*)-**2**, *rac*-**1** and *rac*-**2**). We investigated the structural factors affecting this behaviour by changing the balance between their hydrophilic/hydrophobic moieties (changing the length of their alkyl chain) or the stereochemical composition (enantiomerically pure compounds *vs*. racemic mixtures). For this last purpose, we carried out studies of the structure of the gels, xerogels and monocrystals by means of spectroscopic (IR), microscopic (SEM and AFM) and X-Ray techniques.

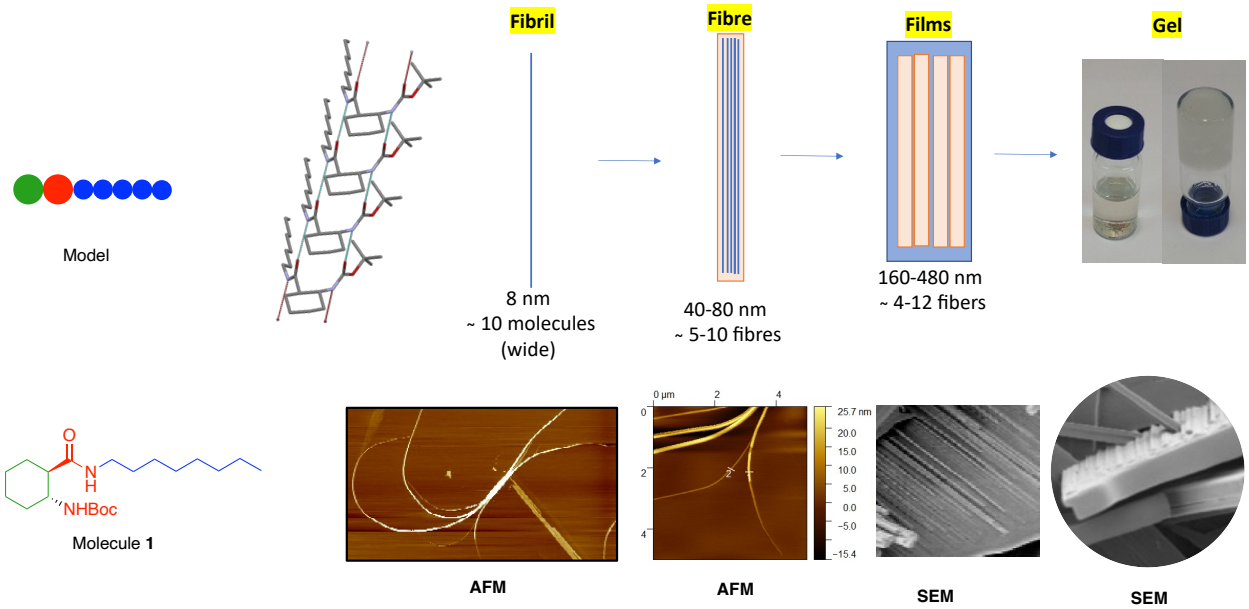

Figure 8: Schematic representation of the hierarchical structuration of *N*-alkylamide gelling agents for the case of compound (1*R*,2*R*)-**1** in hexane.

Monocrystal X-Ray diffraction analysis shows that the individual molecules aggregate unidirectionally to give rise to individual macrostructures stabilized by H-bonds

(Figure 5). Atomic force microscopy (AFM) revealed that these individual structures associate with each other to form fibrils (≈ 2 nm wide) (Figure 3, B), which in turn associate laterally with each other to form wider fibers (Figure 3, C). Finally, scanning electron microscopy (SEM) displays the packing of these fibers to give rise to the lamellar or fibrillar microstructures (Figure 3, A) that support the gel. A model for the hierarchical architecture of the gels here described is summarized in Figure 8.

CONCLUSION

Finding small molecules capable to gelling solvents (LMWGs), and understanding the underlying mechanisms of gelation, are topics of continuing interest in materials chemistry. This work aims not only at describing the excellent gelling capabilities of a new class of LMWGs, in their enantiomerically pure and racemic forms, but also to understand the structural reasons leading to this behavior, which may eventually lead to the design of new and better LMWGs. We present a new gelation system based on *N*-alkylamides derived from cyclohexane β-amino acid that show excellent gelling capabilities of a wide range of solvents. Differences are observed between the gelation ability of the racemic and enantiomerically pure compounds. PXRD experiments performed with gels and xerogels support that the main structural features of the monocrystal structures are conserved in the gels.

Acknowledgements

This work has received financial support from the Spanish Agencia Estatal de Investigación (AEI) and the European Regional Development Fund - ERDF (RTI2018-098795-A-I00), the Xunta de Galicia (ED431C 2018/30, ED431C 2022/21 and Centro singular de investigación de Galicia accreditation 2019-2022, ED431G 2019/03) and the European Union (European Regional Development Fund - ERDF). D.R. thanks Xunta de Galicia for a predoctoral fellowship.

EXPERIMENTAL PART

Materials and instrumentation

Specific rotations were recorded on a JASCO DIP-370 optical polarimeter. Infrared spectra were recorded on a *MIDAC Prospect FT-IR PerkinElmer Spectrum Two* spectrometer. Nuclear magnetic resonance spectra were recorded on Varian Mercury 300, Bruker Avance III 500 and Bruker NEO 750 spectrometers. Mass spectra were obtained on a Kratos MS 50 TC mass spectrometer. X-ray experiments were performed with a Bruker Appex II apparatus. Thin layer chromatography (tlc) was performed using Merck GF-254 type 60 silica gel and ethyl EtOAc/hexane mixtures as eluents; the tlc spots were visualized with a Hanessian stain (dipping into a solution of 12.5 g of $(NH_4)_4Mo_7O_{24}\cdot 4H_2O$, 5 g of $Ce(SO_4)_2\cdot 4H_2O$ and 50 mL of H_2SO_4 in 450 mL of H_2O, and warming). Column chromatography was carried out using Merck type 9385 silica gel. Solvents were purified as in ref. (Perrin, D. D.; Armarego, W. L. F. Purification of Laboratory Chemicals; Pergamon Press: New York, 1988).

Synthesis of (1*R*,2*R*)-1, (1*R*,2*R*)-2, *(3+4), (5+6), rac*-1 and *rac*-2

***tert*-Butyl (1*R*,2*R*)-(2-(octylcarbamoyl)cyclohexyl)carbamate (**(1*R*,2*R*)-**1)**
PyBop (802 mg, 1.54 mmol, 1.5 eq) was added over a solution of acid **5** (250 mg, 1.03 mmol, 1.0 eq) in dry DMF (14 mL) and the mixture was stirred for 30 min. Then, octylamine (510 µL, 3.08 mmol, 3 eq) and DIEA (626 µL, 3.60 mmol, 3.5 eq), were added to the mixture and the reaction was stirred 21 h more under an argon atmosphere. Then, the solvent was removed under vacuum, the residue was redissolved in DCM (5 mL) and washed with 5 mL portions of HCl (1M), NaCl (sat), $NaHCO_3$ (sat.) and NaCl (sat). The organic layer was dried over anhydrous sodium sulphate, filtered, and concentrated under vacuum. The residue was purified by flash column chromatography (EtOAc/Hex 1:1) to afford (1*R*,2*R*)-**1** (228 mg, 93 %) as a white solid.
$[\alpha]_D^{19}$: –23,4° (*c* 1, $CHCl_3$).
^{1}H NMR ($CDCl_3$, 300 MHz, ppm): 0.87 (t, *J* = 6.3 Hz, 3H, CH_3), 1.27 (s, 12H, 6xCH_2), 1.42 (s, 4H, 2xCH_2), 1.58 (s, 9H, $C(CH_3)_3$), 1.75 (s, 2H, CH_2), 1.98 (d, *J* = 13.8 Hz, 2H, CH_2), 2.25 (s, 1H, CHCO), 3.02–3.29 (m, 2H, NCH_2), 3.47 (d, *J* = 9.6 Hz, 1H, CH-N), 4.63 (s, 1H, NH), 6.14 (s, 1H, NH).
^{13}C{^{1}H} NMR ($CDCl_3$, 75 MHz, ppm): 14.17 (CH_3), 22.73 (CH_2), 25.01(CH_2), 25.36 (CH_2), 27.08 (CH_2), 28.48(3xCH_3, Boc), 29.31 (CH_2), 29.40 (CH_2), 29.61 (CH_2), 30.25 (CH_2), 31.92 (CH_2), 33.35 (CH_2), 39.72 (CH_2-N), 51.39 (CH-CO), 51.97 (CH-N), 79.49 (C, Boc), 156.04 (CO, Boc), 174.53 (CO, amide).
HRMS (ESI$^+$): Calculated for $C_{20}H_{39}N_2O_3$, 355.2956; found 355.2955.
IR (cm^{-1}): 3335 (NH, amide A), 1682 (CO, amide I), 1645 (CO, amide I), 1534 (amide II).

***tert*-Butyl (1*R*,2*R*)-(2-(hexadecylcarbamoyl)cyclohexyl)carbamate (**(1*R*,2*R*)-**2)**
Starting from acid **3** (0.1 g, 0.41 mmol) and *n*-hexadecylamine (300 mg, 1.24 mmol), following the same procedure as for compound **5**, compound (1*R*,2*R*)-**2** (165 mg, 86 %) was obtained after purification by flash column chromatography (MeOH/DCM 1:15).
$[\alpha]_D^{20}$: –16,2° (*c* 1, $CHCl_3$).
^{1}H NMR ($CDCl_3$, 300 MHz, ppm): 0.89 (t, *J* = 6.4 Hz, 3H, CH_3), 1.27 (s, 26H, 13xCH_2), 1.46 (s, 11H, $C(CH_3)_3$ + CH_2), 1.57 (m, 2H, CH_2), 1.87 (m, 2H, CH_2), 2.02-2.47 (m, 4H, 2xCH_2), 3.22 (s, 2H, NCH_2), 3.43 (s, 1H, CHCO) 4.24 (s, 1H, NCH), 6.02 (s, 1H, NH), 6.91 (s, 1H, NH).

$^{13}C\{^1H\}$ NMR ($CDCl_3$, 75 MHz, ppm): 14.21 (CH_3), 22.78 (CH_2), 26.98 (CH_2), 28.48 (3xCH_3), 29.39 (CH_2), 29.45 (CH_2), 29.63 (CH_2), 29.69 (CH_2), 29.78 (10xCH_2), 32.02 (CH_2), 39.47 (CH_2), 47.19 (CH_2-N), 60.20 (CH-CO), 61.43 (CH-N), 80.49 (C, Boc), 173 (2xCO).
HRMS (ESI^+): calculated for $C_{28}H_{55}N_2O_3$, 467.4207; found $C_{28}H_{55}N_2O_3$, 467.4207.
IR (cm^{-1}): 3343 (NH, amida A), 1690 (CO, amide I), 1687 (CO, amide I), 1554 (amide II), 1540 (amide II).

Synthesis of methyl (1*R*,2*R*)-2-((*tert*-butoxycarbonyl)amino)cyclohexane-1-carboxylate (9) and methyl (1*S*,2*S*)-2-((*tert*-butoxycarbonyl)amino)cyclohexane-1-carboxylate (10)
Racemic mixture of methyl (1*R*,2*S*)-2-((*tert*-butoxycarbonyl)amino)cyclohexane-1-carboxylate (**7**) and methyl (1*S*,2*R*)-2-((*tert*-butoxycarbonyl)amino)cyclohexane-1-carboxylate (**8**) (330 mg, 1.28 mmol) was added to a dry solution of sodium methoxide 2 M in MeOH (6.5mL) cooled to 0 °C. The mixture was refluxed for 5 h, then cooled to room temperature and 0.5 M aqueous solution of NH4Cl was added. The solvent was removed on a rotary evaporator until a precipitate appears and the formed precipitate was filtered to obtain 247 mg of white solid formed by the two racemic mixtures **7**+**8** (7 %) and **9**+**10** (68 % yield). The two racemic mixtures were recrystallized from n-hexane/DCM (9:1) to afford 225 mg (68 % yield) of racemic mixture **59**+**10** as colorless crystals.

Synthesis of (1*R*,2*R*)-2-((*tert*-butoxycarbonyl)amino)cyclohexane-1-carboxylic acid (5) and (1*S*,2*S*)-2-((*tert*-butoxycarbonyl)amino)cyclohexane-1-carboxylic acid (6)
Racemic mixture of methyl (1*R*,2*R*)-2-((*tert*-butoxycarbonyl)amino)cyclohexane-1-carboxylate (**9**) and methyl (1*S*,2*S*)-2-((*tert*-butoxycarbonyl)amino)cyclohexane-1-carboxylate (**10**) (500 mg, 1.94 mmol) was dissolved in MeOH/H_2O (2:1) (3 mL) and NaOH (233 mg, 5.83 mmol, 3 eq)was then added. The mixture was stirred at room temperature for 15 h, the methanol removed in vacuum and the aqueous residue washed with ethyl acetate (2 x 10 mL). The aqueous layer was acidified with 1 M HCl up to pH 2 and then extracted with ethyl acetate (4 x 10 mL). The organic extracts were dried over MgSO4 and evaporated to give 462 mg (98 % yield) of the racemic mixture **5**+**6** as a white solid.

Synthesis of *tert*-butyl ((1*R*,2*R*)-2-(octylcarbamoyl)cyclohexyl)carbamate and (c**) *tert*-butyl ((1*S,*2*S*)-2-(octylcarbamoyl)cyclohexyl)carbamate (**(1*S*,2*S*)-**3**) (*rac*-1)**
Starting from racemic acid (**5**+**6**) (462 mg, 1.30 mmol), and *n*-octylamine (647 µL, 3.90mmol), following the same procedure as for compound (1*R*,2*R*)-**1**, racemic amide ((1*R*,2*R*)-**1**+(1*S*,2*S*)-**3**, *rac*-**1**) (600 mg, 89 %) was obtained after purification by flash column chromatography (EtOAc/Hex (1:1).

Synthesis of *tert*-butyl ((1*R*,2*R*)-2-(octylcarbamoyl)cyclohexyl)carbamate and ((1*R*,2*R*)-**2**) *tert*-butyl ((1*S,*2*S*)-2-(octylcarbamoyl)cyclohexyl)carbamate (**(1*S*,2*S*)-**4**) (*rac*-2)**
Starting from racemic acid (**5**+**6**) (110 mg, 0.45 mmol) and *n*-hexadecylamine (326 mg, 1.36 mmol) following the same procedure as for compound **1**, racemic amide ((1*R*,2*R*)-**2**+(1*S*,2*S*)-**4**, *rac*-**2**) (198 mg, 94 %) was obtained after purification by flash column chromatography (MeOH/DCM(1:15).

REFERENCES

(1) Seifriz, W. The Structure of Protoplasm. *Science* **1931**, *73* (1902), 648–649. https://doi.org/10.1126/science.73.1902.648.

(2) Banerjee, S.; Das, R. K.; Maitra, U. Supramolecular Gels 'in Action.' *J. Mater. Chem.* **2009**, *19* (37), 6649. https://doi.org/10.1039/b819218a.
(3) de Loos, M.; Feringa, B. L.; van Esch, J. H. Design and Application of Self-Assembled Low Molecular Weight Hydrogels. *Eur. J. Org. Chem.* **2005**, *2005* (17), 3615–3631. https://doi.org/10.1002/ejoc.200400723.
(4) Guenet, J.-M. Physical Aspects of Organogelation: A Point of View. *Gels* **2021**, *7* (2), 65. https://doi.org/10.3390/gels7020065.
(5) Thakur, V.K.; Thakur, M.K. *Polymer Gels: Science and Fundamentals*; Springer Ed., 2018.
(6) Amith, D.K. Molecular Gels: Structure and Dynamics; Royal Society of Chemistry, 2018; pp 300–371.
(7) Terech, P.; Weiss, R. G. Low Molecular Mass Gelators of Organic Liquids and the Properties of Their Gels. *Chem. Rev.* **1997**, *97* (8), 3133–3160. https://doi.org/10.1021/cr9700282.
(8) A. Brizard, R. Oda and I. Huc. *Low Molecular Mass Gelator*; Topics in Current Chemistry; Springer Berlin Heidelberg: Berlin, Heidelberg, 2005; Vol. 256. https://doi.org/10.1007/b105250.
(9) McAulay, K.; Dietrich, B.; Su, H.; Scott, M. T.; Rogers, S.; Al-Hilaly, Y. K.; Cui, H.; Serpell, L. C.; Seddon, A. M.; Draper, E. R.; Adams, D. J. Using Chirality to Influence Supramolecular Gelation. *Chem. Sci.* **2019**, *10* (33), 7801–7806. https://doi.org/10.1039/C9SC02239B.
(10) Ghosh, D.; Farahani, A. D.; Martin, A. D.; Thordarson, P.; Damodaran, K. K. Unraveling the Self-Assembly Modes in Multicomponent Supramolecular Gels Using Single-Crystal X-Ray Diffraction. *Chem. Mater.* **2020**, *32* (8), 3517–3527. https://doi.org/10.1021/acs.chemmater.0c00475.
(11) Kim, J.-U.; Schollmeyer, D.; Brehmer, M.; Zentel, R. Simple Chiral Urea Gelators, (R)- and (S)-2-Heptylurea: Their Gelling Ability Enhanced by Chirality. *Journal of Colloid and Interface Science* **2011**, *357* (2), 428–433. https://doi.org/10.1016/j.jcis.2011.02.006.
(12) Pasteur, L. *Recherches Sur Les Relations Qui Peuvent Exister Entre La Forme Crystalline, La Composition Chimique et Le Sens de La Polarisation Rotatoire*, Ann. Chim. Phys.; 1848; Vol. 24.
(13) Ortuño, R. M. Carbocycle-Based Organogelators: Influence of Chirality and Structural Features on Their Supramolecular Arrangements and Properties. *Gels* **2021**, *7* (2), 54. https://doi.org/10.3390/gels7020054.
(14) Hanabusa, K.; Yamada, M.; Kimura, M.; Shirai, H. Prominent Gelation and Chiral Aggregation of Alkylamides Derived Fromtrans-1,2-Diaminocyclohexane. *Angew. Chem. Int. Ed. Engl.* **1996**, *35* (17), 1949–1951. https://doi.org/10.1002/anie.199619491.
(15) Pi-Boleda, B.; Sans, M.; Campos, M.; Nolis, P.; Illa, O.; Estévez, J. C.; Branchadell, V.; Ortuño, R. M. Studies on Cycloalkane-Based Bisamide Organogelators: A New Example of Stochastic Chiral Symmetry-Breaking Induced by Sonication. *Chem. Eur. J.* **2017**, *23* (14), 3357–3365. https://doi.org/10.1002/chem.201604818.
(16) Pi-Boleda, B.; Campos, M.; Sans, M.; Basavilbaso, A.; Illa, O.; Branchadell, V.; Estévez, J.; Ortuño, R. Synthesis and Gelling Abilities of Polyfunctional

Cyclohexane-1,2-Dicarboxylic Acid Bisamides: Influence of the Hydroxyl Groups. *Molecules* **2019**, *24* (2), 352. https://doi.org/10.3390/molecules24020352.
(17) Estroff, L. A.; Hamilton, A. D. Water Gelation by Small Organic Molecules. *Chem. Rev.* **2004**, *104* (3), 1201–1218. https://doi.org/10.1021/cr0302049.
(18) Le Bail, A. Whole Powder Pattern Decomposition Methods and Applications: A Retrospection. *Powder Diffr.* **2005**, *20* (4), 316–326. https://doi.org/10.1154/1.2135315.